

Preparation of Conductive and Semiconductive Patterns by Digital Printing of Nanodispersions for Sensing Devices of Organic Compound Vapours

Ing. Jan Mašlík, Ph.D.

Doctoral Thesis Summary



Tomas Bata University in Zlín

Faculty of Technology

Doctoral Thesis Summary

Preparation of Conductive and Semiconductive Patterns by Digital Printing of Nanodispersions for Sensing Devices of Organic Compound Vapours

**Příprava vodivých a polovodivých vzorů digitálním tiskem
nanodisperzí pro senzory par organických látek**

Author: **Ing. Jan Mašlík, Ph.D.**

Study programme: Chemistry and Materials Technology (P2808)

Study course: Technology of Macromolecular Compounds (2808V006)

Supervisor: Assoc. Prof. Ing. *et* Ing. Ivo Kuřitka, Ph.D. *et* Ph.D.

Consultant: Ing. Michal Machovský, Ph.D.

External examiners: Prof. Ing. Mohamed Bakar, PhD,
Assoc. Prof. Petr Filip,
Prof. Ing. Petr Slobodian, Ph.D.

Zlín, June 2019

© Jan Mašlík

Published by **Tomas Bata University in Zlín** in the Edition **Doctoral Thesis Summary**.

The publication was issued in the year 2019

Key words in English: *ink-jet printing, flexible electronics, printed conductors, nanoparticle ink, sensors*

Key words in Czech: *inkoustový tisk, flexibilní elektronika, tištěné vodiče, nanočásticový inkoust, senzory*

Full text of the doctoral thesis is available in the Library of TBU in Zlín.

ISBN 978-80-7454-849-9

ACKNOWLEDGEMENT

First and foremost, I would like to thank my family: my parents and sister for supporting me spiritually and financially throughout doctoral study, writing the thesis and my life in general.

I would like to also express my sincere gratitude to my supervisor

Assoc. Prof. Ing. et Ing. Ivo Kuřitka, Ph.D. et Ph.D. for an opportunity to become a member of his research team, possible access to a variety of instrumentation and equipment, the continuous support during my Ph.D. study and related research and project work, for his strict approach but also patience, mentoring and immense knowledge.

Besides my supervisor, I would also like to thank my consultants Ing. Michal Machovský, Ph.D. for his assistance and contribution and Ing. Pavel Urbánek, Ph.D. for the stimulating discussions and encouragement all along doctoral study.

A very special gratitude goes out to all members of Functional Nanomaterials Research Group at Centre of Polymer Systems of Tomas Bata University in Zlín, namely: Ing. Pavol Šuly, Ph.D., Ing. Petr Krčmář, Ing. Jan Antoš,

Ing. Jakub Ševčík, Ing. Milan Masař, Ing. Lukáš Münster, Ph.D., Ing. Barbora Hanulíková, Ph.D., Ing. Michal Urbánek, Ph.D., Mgr. Jan Vícha, Ph.D., Raghvendra Singh Yadav Dr., M.Sc. Thaiskang Jamatia and M.Sc. David John Dmonte.

My sincere thanks also go to Tomas Bata University in Zlín, Faculty of Technology for the provided education and Centre of Polymer Systems for granted facility, equipment, financial support, and working environment.

This dissertation work was supported and founded by the Ministry of Education, Youth and Sports of the Czech Republic—Program NPU I (LO1504), Operational Program Research and Development for Innovations co-funded by the European Regional Development Fund (ERDF) and national budget of Czech Republic, within the framework of project CPS—strengthening research capacity (reg. number: CZ.1.05/2.1.00/19.0409), and Internal Grant Agency of Tomas Bata University in Zlín, grant No., IGA/FT/2014/006, and IGA/CPS/2015/006 in which I was working as a head of research team, and grant No. IGA/FT/2013/025, IGA/CPS/2016/007, and IGA/CPS/2017/008, in which I was working as a member of the research team.

And finally, last but by no means least, to everybody who made possible this small contribution to science.

TABLE OF CONTENTS

1. INTRODUCTION.....	1
2. INK-JET MATERIAL PRINTING.....	3
2.1 Continuous Ink-jet	3
2.1 Drop-on-demand Ink-jet	4
3. INK FORMULATION.....	5
4. INK-JET PROCESS PARAMETERS	6
4.1 Ink parameters.....	6
4.2 Tool parameters.....	6
4.3 Process parameters.....	7
4.4 Dimensionless correlations of the parameters and drop generation	7
5. SELECTED APPLICATIONS	9
5.1 Conductive interconnects for electric circuits	9
5.2 Gas sensors.....	9
6. AIM OF DOCTORAL THESIS.....	10
7. EXPERIMENTAL	11
7.1 Materials and methods	11
Preparation of conductive interconnects	11
Water-based Indium Tin Oxide Nanoparticle Ink for Printed Toluene Vapours Sensor Operating at Room Temperature	11
Development of ZnO nanowire-based gas sensor using ink-jet printing.....	12
8. SUMMARY OF RESULTS, DISCUSSION AND CONCLUSIONS	14
9. SUMMARY OF CONTRIBUTIONS TO SCIENCE AND PRAXIS.....	26
REFERENCES	28
LIST OF FIGURES	32
LIST OF TABLES.....	33
LIST OF ABBREVIATIONS	34
LIST OF SYMBOLS.....	35
LIST OF DIMENSIONLESS NUMBERS	36
LIST OF UNITS	37
LIST OF PUBLICATIONS.....	38
CURRICULUM VITAE.....	41

ABSTRACT

To simplify, accelerate, and facilitate production processes, ink-jet technology appears to be a very effective and inexpensive alternative to conventional deposition methods. Nowadays, it is rapidly developing in electronics, with the help of conductive polymers and various materials in the form of nanoparticles. The thesis deals with inkjet printing technology as a deposition technique of functional materials in the form of thin films and their applications. The literature review covers the current state and possibilities of inkjet technologies, as well as the used materials, their compatibility with the printing equipment, the fabrication process, and the final application. First, it was necessary to optimize the fabrication of conductive interconnects from silver nanoparticles on flexible polymer foils. Then, ITO (indium tin oxide) nanoparticle ink was developed and characterized for application in sensing devices detecting vapours of the organic volatile compounds. As a side product of this work, a framework for ink and inkjet printing process optimization using dimensionless criteria was developed.

The last part of presented results is devoted to the successful development of a ZnO nanowire forest hydrothermal deposition method and their utilization in preparation of the IDE designed printed sensor on a polymer substrate. Then, the same technique was applied for developing a novel low temperature operated miniature gas sensing device prepared directly on the top of the quartz window of a UV emitting LED using UV activation of the semiconducting ZnO sensing layer replacing high-temperature activation.

ABSTRAKT

Pro zjednodušení, zrychlení a usnadnění výrobních procesů se jeví technologie inkoustového tisku jako velmi efektivní a nenákladná. Z tohoto důvodu se v současnosti rychle rozvíjejí především v oblasti elektroniky, s využitím nejrůznějších vodivých polymerů a materiálů ve formě nanočástic. Práce se zabývá technologií inkjetového tisku a jejího využití v depozici funkčních materiálů ve formě tenkých vrstev a jejich aplikací. Literární část obsahuje aktuální stav a možnosti inkoustových technologií stejně jako používané materiály a jejich kompatibilitu s tiskovým zařízením, výrobním procesem a výslednou aplikací. Nejprve bylo nutné optimalizovat přípravu vodivých cest ze stříbrných nanočástic na ohebných polymerních foliích. Poté byl vyvinut inkoust z ITO (indium cín oxid) nanočástic a charakterizován pro aplikaci v senzorech detekujících páry těkavých organických sloučenin. Jako další výsledek byla rozpracována metoda vývoje inkoustu a procesu tisku pomocí bezrozměrných kritérií. Poslední část prezentovaných výsledků je věnována úspěšnému vyvinutí hydrotermální metody depozice ZnO nanodrátkových polí a jejich využití v přípravě tištěného senzoru s designem interdigitálních elektrod na polymerním substrátu. Poté byla ta samá technika použita pro vývoj nového nízkoteplotně provozovaného miniaturního senzoru plyných látek připraveného přímo na křemenném okénku UV emitující LED a využívajícího tak UV aktivaci polovodičové ZnO sensorické vrstvy nahrazující aktivaci zvýšenou teplotou.

1. INTRODUCTION

Material printing technologies (including screen-printing, roll-to-roll printing, gravure printing and ink-jet printing) are widely used especially in graphics and marking industry, however nowadays, the printing technology offers the possibility of applications in electronics (fabrication of conductive circuits and interconnects, solar cells, light-emitting and sensing devices, antennas, membranes etc.). Their advantageous application leads to accelerating and efficient production, reducing production costs and also the versatility of final products which can turn it into a commodity soon. [1]

These low-cost technologies are based on depositing functional materials onto a used substrate such as glass or transparent and flexible polymer foils, textile materials, ceramics or metal wafers. Unlike other printing methods, ink-jet printing does not require any master form, stencils or masks; therefore, it allows instantaneous and rapid designs and prototyping with no delay between the digital motive generation and material deposition. The ink-jet printing is an interesting and versatile method to make controlled and localized deposition of functional materials with suitable geometry on various substrates at low processing temperatures. [1-4] The printed patterns are designed by common computer programs and can be saved as simple bitmap images for printing. It is possible to use a wide range of inorganic and organic materials, including inks based on metal or metal oxide nanoparticles and polymer solutions. [4-7] The size of used nanoparticles, their dispersion in a proper liquid medium and a suitable dispersion stabilization, viscosity and the surface tension of the ink composition for jetting are vitally important and challenging parameters to be developed for the required flow of the ink through the nozzles of a printing head yielding the proper generation and ejection of droplets, which is the limiting factor of this material deposition printing process.

Mentioned advantages predict ink-jet printing a suitable technology for depositing both conductive interconnects using metal nanodispersions, as well as active and passive elements from functional materials in the field of polymer electronics and sensors. Printing of inks based on silver nanoparticles (Ag NPs) enables low-cost deposition of precisely defined conductive tracks on a wide range of substrates. The ink-jet printing of Ag NPs inks can be performed at room temperature and without residual waste.

Together with conductive interconnects, it is also possible to print and form functional layers having semiconducting properties which jointly construct advanced devices such as various sensors and detectors. Especially, with regard

to the environment, sensors monitoring air quality and detecting the threat of contamination of irritant, harmful fumes and gases are of particular interest.

For this purpose, metal oxides (among them indium tin oxide – ITO and zinc oxide being the most widely used) are indispensable materials in the fabrication of optoelectronic devices and can be used as a semiconductive material for gas detecting sensors based on the resistance variation due to its exposure to the target gas. Films made from ITO ($\text{In}_2\text{O}_3:10 \text{ wt}\% \text{ SnO}_2$) and ZnO have been extensively studied in recent years and the applicability of these semiconductors as an active thin film of sensor device deposited by various techniques (such as the thermal evaporation technique, sputtering, screen–printing) has been widely reported with respect to sensing reducing and oxidizing gases and organic compounds (NH_3 , CO, H_2 , NO_2 , toluene etc.). [4,8-13] Indium tin oxide and zinc oxide react depending on ambient atmosphere composition by changing the electrical conductivity due to the presence of oxygen vacancies. [9] Electrical conductivity is transferred as a signal of the electrical resistance variation of the deposited film upon the introduction of reducing or oxidizing gases. The signal is a function of the partial pressure of target gas. [8-12]

2. INK-JET MATERIAL PRINTING

Ink-jet printing involves several partial processes from the material deposition point of view. These include preparation and characterization of the printed fluid (allowing its compatibility with the substrate surface), layout and designing of the desired motifs, the printing process parameters setting and characterization of deposited structures. Material jetting consists of releasing fluid in the form of small droplets from the cartridge through the print head nozzles. The drops are deposited in a precise location on the surface of the substrate. Each drop forms an equilibril spherical cap after impact on its position. Thus, a single dot of material is formed after drying of the ink. Due to the overlap and coalescence of drops on the surface and appropriately set drop spacing, uniform films can be formed. Ink-jet printing is further divided according to the principle by which drops are formed and deposited. Dominant modes of drop generation are continuous ink-jet (CIJ) and drop-on-demand ink-jet (DOD). [2,14,15]

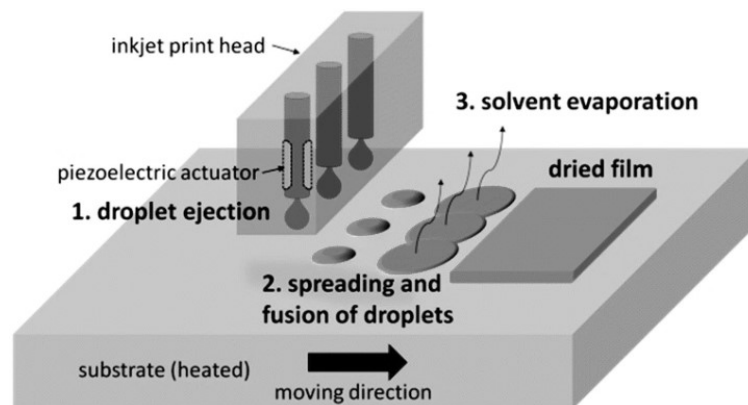


Fig. 1: Thin film formation using material ink-jet printer. Adopted from [31]

2.1 Continuous Ink-jet

Recently, different methods of continuous ink-jet (CIJ) printing have been developed and commercialized. In general, continuous ink-jet system jets energetically unstable stream of liquid from a high-pressurized ink reservoir. This free surface stream is subsequently break up into drops. Due to a periodic stimulus applied by a vibrating piezoelectric transducer at the orifice of the printing nozzle, it is possible to synchronize the breakup of each drop and to generate a steady stream of droplets having the same size, period (spacing between drops) and velocity. [2,16-19] Certain drops are subsequently charged and deflected from a continuous stream passing through fixed high-voltage electrode plates to separate printing drops from nonprinting drops. Depending on the used technology, non-

or deflected droplets land at the right place on a substrate to form the printing. The rest of unused drops is collected in a gutter and recirculated. [20-24]

2.1 Drop-on-demand Ink-jet

The main characteristic feature of the drop-on-demand (DOD) ink-jet printing in comparison with CIJ printing is activation of each micronozzle individually to produce pressure pulse inside the ejection chamber to generate well-defined volume and velocity of drops. Basically, the DOD technology can be divided into two distinct branches according to the principle of ink drop generation. The ink ejection and drop formation are most often driven by a piezoelectric transducer or by a thin-film resistive heater integrated into a wall of separated nozzle chambers and it is software-configurable as required.

Piezoelectric Drop-on-demand Ink-jet

Voltage-driven piezoelectric transducers (based on lead zirconium titanate – PZT) converts applied voltage to mechanical deformation of separated ejection chambers of a printing head. Piezo element adjacent to / or placed inside of the ejection chamber mechanically deforms its walls and generate pressure pulse inside. Generated pressure pulse in the fluid filled inside of ejection chamber feed a nozzle and force a fluid to be ejected. Switching polarity of applied voltage alter the volume of the chamber and thus, raises or reduces the pressure inside. Applied voltage waveform tunes time-dependent pressure pulses optimizing well-defined volume and velocity of drop ejection and subsequently refills the chamber. A fluid inside the ejection chamber is contained at the orifice held by surface tension preventing spontaneous leaking. If the critical value of the surface tension is exceeded due to the applied pressure pulse, the liquid begins to separate through a neck forming as a droplet. [2,18,25-27]

Thermal Drop-on-demand Ink-jet

A defined drop jetting is possible to control by thermal pulses applied inside of ejection chamber. Integrated thin-film resistive heater, activated by short-duration voltage pulses, raises the temperature of a thin layer of ink (up to 300 °C), which evaporates explosively and produces a vapour bubble. The rapid expansion of the bubble inside the chamber leads to ejection of the ink through the nozzle and forms a droplet of desired volume and velocity. Then, the heat pulse is removed allowing the ejection chamber to be refilled from an ink reservoir [14,28,29].

3. INK FORMULATION

A crucial operation of the entire printing process is the preparation of a material being printed, which is required to be in the form of a liquid dispersion, i.e. an ink. The ink composition affects both the printing process and the properties of printed structures and hence a device. Parameters of the final printed layers are necessary to be considered while preparing the ink composition which has to meet all necessary chemical and physicochemical criteria to assure compatibility of the ink with the substrate, jetting performance and storage stability. It is a multidimensional parameter space which must be researched and where an optimum must be found. The crucial fluid parameters enabling optimal printability are therefore ink density, viscosity, surface tension, the stability of the suspension and the size of the nanoparticles, which is partially related to the operating performance of the device. [4,6,30]

Ink preparation requires several steps involving optimizing their composition corresponding to the printer's process parameters. Figure 2 shows the generally used components and their requirements relating to inks containing functional materials and layers deposited thereon.

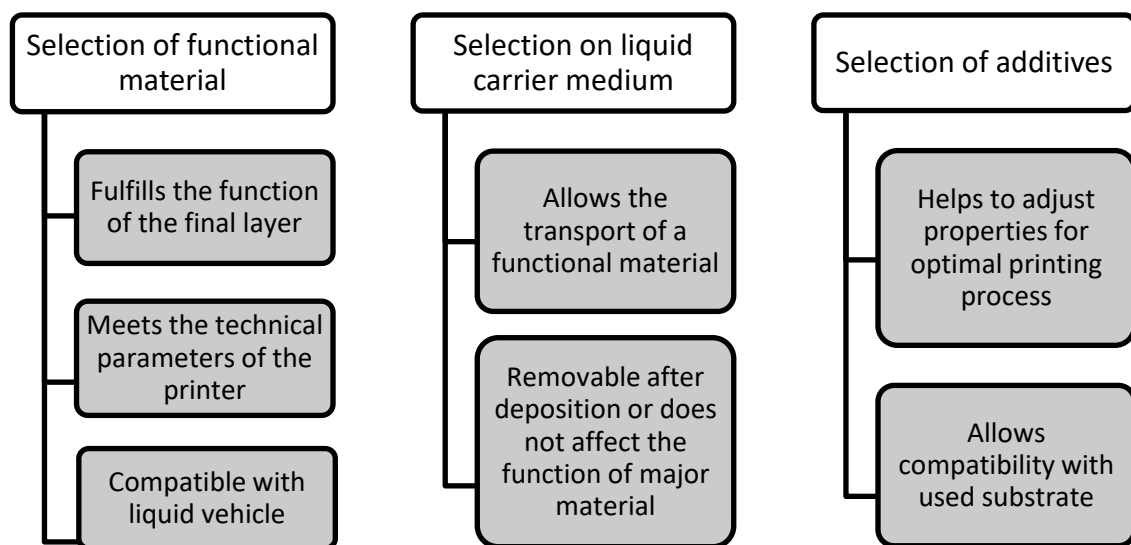


Fig. 2: Ink components and requirements

With regard to inks be composed of functional particles, their size must be considered relating to the technical parameters of an ink-jet printer which reach their limitations in terms of particle transport through the print head nozzle, but also because of the stabilization in the dispersing medium. Printer specifications

enable deposition of particle size smaller than 1/10 of the nozzle diameter as a rule of thumb, which is critical to avoid clogging and therefore, particle size smaller than 1/50 or even 1/100 [31] is preferable. Considering the diameter of the nozzles which is in the order of tens of micrometres, then, micro- and nanometer-sized particles are optimal. [2,3,6,7]

4. INK-JET PROCESS PARAMETERS

The printing process requires compatibility of parameters of the ink, the printing apparatus and process conditions. Therefore, the ink parameters must be considered prior to the printing process as already mentioned in chapter 3. Individual parameters of the ink, processing velocity and ink-jet tool and their relation are described in this chapter. Interaction between the ink and the substrate surface is also related to the resulting quality and precision of printed shapes.

4.1 Ink parameters

Properties of the inks are the most important factor influencing almost all steps of the entire printing process. Requirements for ink properties, namely viscosity and surface tension are specified by the printer manufacturer. Density and ink stability should meet required specifications also. These bits of advice should be followed for optimal printing performance and high quality of printed motifs. On the other hand, the fulfilment of these criteria does not automatically assure good printability of the ink. The overall performance of the printing of ink is determined by the function of the final thin-film structure. In case the thin-film feature is adversely affected, it is necessary to identify which one of the ink parameters causes these errors and then, tune the ink composition adequately, which actually is the ‘trial – error’ method. [6]

4.2 Tool parameters

The main tool-related parameter playing role in the ink-jet printing process is the nozzle diameter which may be considered as a good approximation of the fluid stream diameter, hence its characteristic length. If the geometry of the nozzle’s orifice differs from the circular one, the characteristic length A is derived as an equivalent (hydraulic) diameter by a general formula:

$$A = 4 \cdot \frac{S}{O} \quad (1)$$

where S is the area of the nozzle, and O is its wetted perimeter. In case of a square, A equals to the size of its side. [32]

4.3 Process parameters

There are two main parameters in ink-jet printing which influences the process of drop generation. The temperature may be considered as an external condition, while the fluid flow velocity is a parameter of prime importance which has a direct impact on the process. As the temperature has an impact on viscosity and surface tension of printed liquid vehicle, which has to be taken into account during the printing deposition process, it needs to be precisely controlled in experimental work, as well as in real applications.

Nevertheless, fluid ejection velocity is a parameter which can be varied to a large extent and directly controls the process of ink drop formation and its deposition on the substrate. The piezoelectric element giving momentum to the fluid is driven by the voltage pulse waveform. The waveform is divided into several segments representing a sequence of programmed voltage steps resulting in the sequence of events of the ink fluid ejection from the printing head's nozzle. The fluid ejection velocity is controlled by the steep increase of voltage deflecting the piezoelectric element which decreases the volume of the nozzle chamber quickly thus generating pressure that expels the fluid out of the chamber. In such way, the drop velocity can be varied from a few $\text{m}\cdot\text{s}^{-1}$ up to $15 \text{ m}\cdot\text{s}^{-1}$ for the printer used in this work. A good velocity to set is about $6 \text{ m}\cdot\text{s}^{-1}$. [2,3,6,14]

4.4 Dimensionless correlations of the parameters and drop generation

The drop generation in drop on demand piezoelectric ink-jet printing is a repeated cycle process. The cycle can be described in five steps: (1) ejection and stretching of liquid forming thus a liquid thread – a free surface flow, (2) pinch-off of the liquid thread from the nozzle orifice, (3) contraction of the liquid thread, (4) breakup of the liquid thread into primary drop and satellites, and (5) recombination of primary and satellite drops. In an ideal case, no breakup appears and a single spherical drop is formed in the last (fourth) step. Finally, the drops land on the substrate after travelling through the whole standoff distance. [14,33]

Suitable correlations between the viscosity, the surface tension, and the density of inks, the characteristic length as the tool parameter, and the fluid velocity as the main variables influencing the success of the ink-jet printing at given conditions. The composition and properties of used inks with a used ink-jet printer

characteristics and processing parameters can be analysed rationally with the use of dimensionless criteria, namely by the Reynolds (Re), the Weber (We), the Capillary number (Ca), the Ohnesorge (Oh) number, and the number Z . The number Oh^2 is known as the Laplace number (La). Generally, the printability range used to be determined by a Z number, which is the inverse of the Ohnesorge number (Oh). The recommendations for the optimum range of the Z number vary, however, it was found that the Z number (or obviously Oh number too) alone is insufficient for describing the droplet formation dynamics because all the terms describing dynamic effects are cancelled in its formula and only the material constants and characteristic length remain. [4,33] Thus, other important non-dimensional parameters such as the Reynolds number (Re), the Weber number (We), and the capillary number (Ca) should also be taken into consideration to complete the material-process-tool parameter-related triad. A plot of two suitable selected dimensionless numbers should be enough to map the parameter space for Newtonian fluids. A good example may be found in the work of McKinley and Renardy [34], who replotted a diagram originally constructed by Derby [35]. A schematic in Figure 3 adopted from their works shows the operating regime for stable and printable fluids in drop-on-demand ink-jet printing indicating also the adverse effects outside of the good printability area.

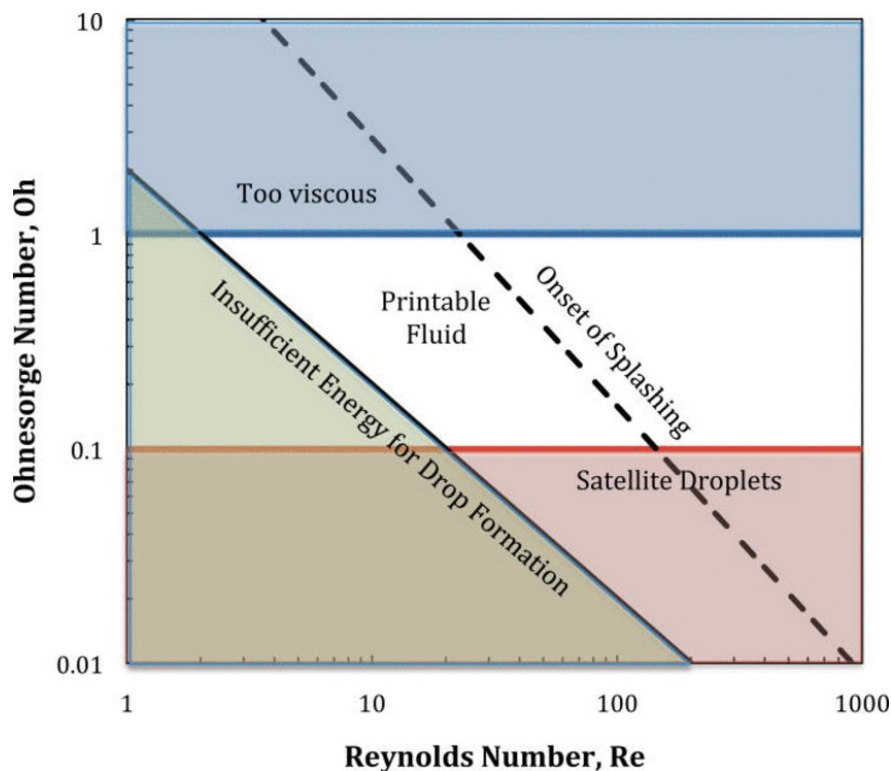


Fig. 3: Ink suitability using dimensionless criteria. Adopted from [34]

5. SELECTED APPLICATIONS

5.1 Conductive interconnects for electric circuits

The deposition of conductive structures in microelectronics is one of a wide range of ink-jet application. Digital ink-jet printing enables the integration of components and electronic elements in the form of *printed wiring*. In combination with soldering, glueing and mounting allows assembling of circuit boards and other hybrid printed integrated circuits. It is also widely used for deposition of electrode and RFID structures as the basis of antennas and other advanced scanning devices. [36-40]

5.2 Gas sensors

Gas sensing devices are capable to provide information about the environmental and chemical composition of ambient conditions and are an indispensable part of testing facilities monitoring workplace hygiene in chemical processes, mining industries, as well as hospitals, schools and houses. Hence, gas sensors are in the centre of interest of this thesis especially for their simplicity both in terms of fabrication and operation.

Three levels of view of gas sensors can be used. From the first point of view, the sensor can be considered as a device able to respond to various nonelectrical stimuli transducing them into an electrical signal whose magnitude is functionally related to the concentration of the analyte and the device generates electrical output directly. [41-44] The second point of view already assumes a semiconducting metal oxide in the form of a thin layer based on nanoparticles as the active sensing material having overall conductivity/resistance value. The detection of various gases and vapours and their concentration is possible due to the change of conductivity of the active sensing material upon adsorption or desorption of the gas on the surface of active material. The change in conductivity is manifested macroscopically as a change of the device's conductance/resistance accordingly. The third view looks into the structure of the layer made up of nanoparticles having intrinsic resistance, the resistance given by the boundaries between them and the chemical reactions in which the charge carriers are transferred between the material of active layer and the detected gas molecules. The ability of the gas sensor to detect harmful substances is therefore determined by the concentration of the transferred charge carriers and their mobility within the active layer. [41,45,46]

6. AIM OF DOCTORAL THESIS

The work aims at original preparation of sensors as representative electronic devices fabricated by using of material ink-jet printing technique from both originally prepared or commercially available nanoparticles-based and solution-based inks. The structure, morphology and properties of deposited materials and prepared devices are investigated with respect to their function.

This aim may be achieved by the accomplishment of the following objectives:

- Adoption and mastering of the preparation of conductive interconnects and electrodes by the ink-jet printing using silver nanoparticles-based inks. Particular attention shall be paid to printing on polymer foils applicable in flexible electronics.
- Research and development of ink based on metal oxide nanoparticles (ITO), its deposition using ink-jet printing technique on a suitable substrate and observing and evaluating the response of printed devices to the presence of volatile organic compounds vapours (e.g. toluene). The sensor is intended for low (ambient) temperature operation. Therefore, the sensing mechanism at low temperature shall be elucidated. In order to develop the ink and optimize the printing process in a rational and well-considered manner, printability evaluation approaches based on dimensionless criteria shall be reinterpreted.
- Research and development of advanced sensing devices based on a semiconductor nanowire network prepared using ink-jet printing technique and integrating previous achievements of the work. The device shall be designed in order to unlock further improvement of sensitivity to detect organic vapours and gases at room operating temperatures.

7. EXPERIMENTAL

7.1 Materials and methods

Deposition method

Functional materials in the form of inks were deposited using material ink-jet printer FUJIFILM Dimatix DMP-2800 series. Printing nozzle orifice has square shape with the size of its side 21.5 μm which is a fixed characteristic (equivalent diameter) of the used 10 pl nominal drop size printing head cartridge having 16 nozzles. The fluid ejection process and namely drop velocity were controlled by waveform setup individually for each nozzle in the printing head.

Preparation of conductive interconnects

Silver nanoparticles-based inks DGP 40LT-15C (Ink 1) and DGH 55LT-25C (Ink 2) (ANP Co., South Korea), were selected for printing on polymeric foils. Polyimide (PI) foil Upilex-50S (UBE Industries, Japan) and polyethylene terephthalate (PET) foil Tenolan OA 0006 (Fatra, a.s., Czech Republic) were used as substrates for final model devices. Microscope glass slides (ThermoFisher Scientific) were used as reference substrates for dimensional and electrical characterization.

Water-based Indium Tin Oxide Nanoparticle Ink for Printed Toluene Vapours Sensor Operating at Room Temperature

ITO nanoparticle-based aqueous inks were prepared in the form of dispersions. Indium tin oxide nanopowder < 50 nm particle size (Sigma-Aldrich spol. s r.o., Prague, Czech Republic) was mixed with the optimum ratio of a polymeric dispersing agent and silicon surfactant provided by BYK-Chemie, ALTANA (Disperbyk®-190 and Byk®-348). The concentration of both these additives was set to be slightly above their CMCs. Ethylene glycol was chosen for modifying the density and viscosity of the dispersion (Sigma-Aldrich product). The dispersions were mixed for several hours in a sealed flask and were sonicated for 30 min by UZ Sonopuls HD 2070 homogenizer and filtered through a 0.22 μm PTFE filter to remove aggregates and agglomerated particles before filling the cartridge (n.b.). The concentrations of the ITO nanoparticles in the prepared inks were set to 10, 15, 20 and 25 wt% to compare the overall performance of each.

The films were deposited by material ink-jet printer FUJIFILM Dimatix DMP-2800 series and made by one printing run (one layer).

The printed films were dried in an oven at 60 °C for 30 min and then annealed in a muffle furnace. Then, copper wires were mounted with contact electrodes

which were deposited manually by the highly conductive silver paste COATES XZ250, dried at 120 °C for 20 min in oven. Prepared sensing devices were connected to a measuring unit. [4]

Development of ZnO nanowire-based gas sensor using ink-jet printing

Conductive interdigitated electrodes were printed using silver nanoparticles ink DGH 55LT-25C on polyimide foil Upilex-50S.

Zinc acetate dihydrate $\text{Zn}(\text{CH}_3\text{COO})_2 \cdot (\text{H}_2\text{O})_2$ (Penta Chemicals) was dissolved in ethanol for UV spectroscopy grade $\geq 99.8\%$ (Penta Chemicals) at 50 °C for 1 hour to form a particle-free solution with concentration of 10 mM, filtered through 0.22 μm pore PTFE syringe filter before filling the cartridge and locally printed as a precursor material onto (i) interdigitated electrode structures of flexible polyimide foil and (ii) a commercial SMD UV-LED (Roithner Lasertechnik GmbH, Austria) operating at $\lambda = 365\text{ nm}$.

After the deposition, films were thermally decomposed at (i) 250 °C for 10 minutes in a muffle furnace (Nabertherm™, Germany) and (ii) 5 minutes on a hot plate (to keep limitation of mount device) to form ZnO quantum dots as nanowire seeds. Subsequently, films were subjected to hydrothermal growth in a bath of three different concentrations of a growth-direct agent consisting of polyethylenimine, ethylenediamine branched (Sigma-Aldrich product) at 92 °C for 24 hours.

Sensor performance characterization

The response of sensors consisting of indium tin oxide layer was measured using multimeter UNI-T HC-UT71D with interface software that records observed resistance. To reach the goal in chapter 6.1.2, changes between “On” and “Off” sensor states upon exposure to vapours of toluene and removal from the vapours were measured. Experiments were carried out at the ambient atmosphere in the laboratory and in a nitrogen atmosphere (less than 1 ppm of O_2 and H_2O) in the glove box GP Campus (Jacomex). In chapter 6.1.3, Response of sensors were measured using customized gas sensing measurement setup as schematically describes Figure 4. The amount of carrier gas was accurately controlled by arranging of mass flow controllers EL-FLOW Prestige (Bronkhorst High-Tech BV, Netherland). Precise dosing of targeted organic substance represented by ethanol was carried out manually by microliter syringe (Hamilton, USA) and transferred through the evaporating unit into a gas chamber. Sensor devices were plugged in 4-pin stripe connector placed inside the gas chamber for easy and fast sample installation and without the need for soldering. Two terminals of stripe connector were used for logging the resistance and remaining

two terminals supplied a UV-LED element. Resistance changes of the sensor devices were measured and logged using multimeter UNI-T HC-UT71D with interface software. The temperature inside the gas chamber was monitored using platinum temperature sensor PT100.

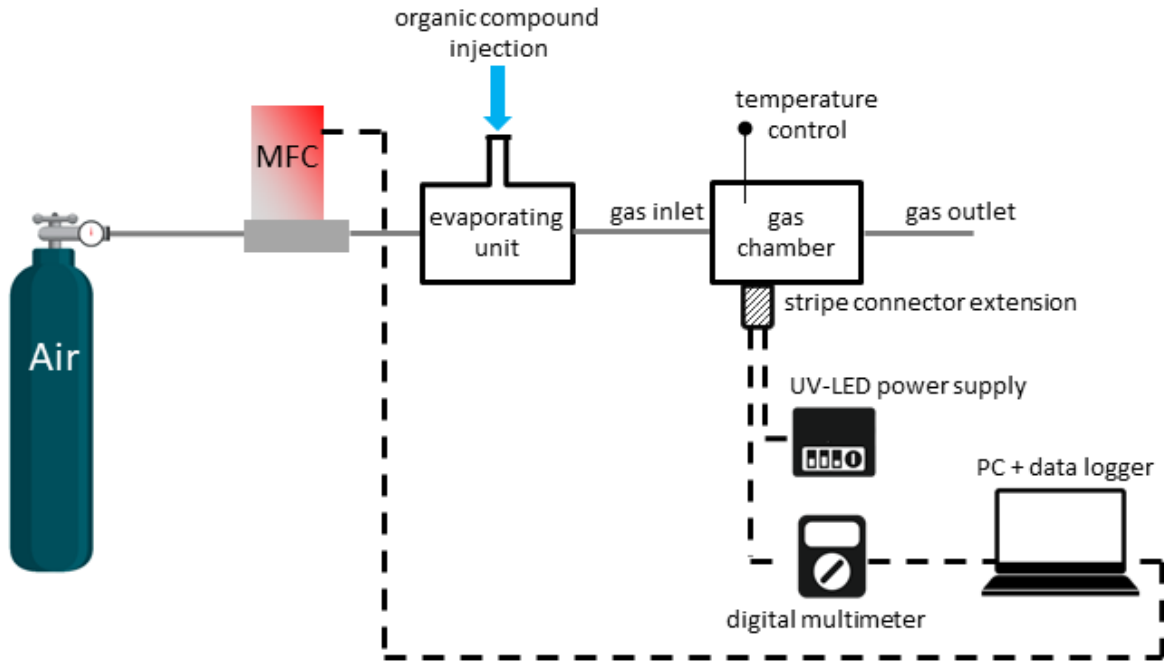


Fig. 4: Schematic illustration of gas sensing measurement setup

The measured electrical resistance is calculated as a sensor response ratio S_R expressed as a percentage as defined [12]:

$$S_R (\%) = \left(\frac{R_{gas}}{R_{air}} - 1 \right) \cdot 100\% \quad (2)$$

where R_{air} represents the sensor resistance in the air free of vapours atmosphere conditions and R_{gas} resistance upon exposure of ambience or carrier gas with targeted vapours. [4]

8. SUMMARY OF RESULTS, DISCUSSION AND CONCLUSIONS

Results corresponding to objectives defined in the aim of the doctoral thesis include the preparation and characterization of functional materials in the form of inks for the material ink-jet deposition of simple conductive interconnects, structures with sensing properties and nanostructured thin films, their characterization and applicability in gas sensor devices.

Deposition of continuous layers

The size of the deposited drops determines and limits the dimensions of the formed structures. Depending on the size of individual deposited drops, the *drop spacing* is selected indicating the distance between the centres of individual drops deposited in a row behind. Due to overlapping and coalescing of drops after the deposition, a continuous conductive interconnect is formed.

Characterization of electric properties

Resistivity characterization of silver conductive interconnects took place on the basis of two-point resistance measurement of pixelated lines array (see Figure 5) printed on a glass slide as a reference substrate. The Ink 1, which is intended for printing on the PET foil, was cured at 150 °C and the Ink 2, which is intended for printing on the PI foil, was cured at 250 °C, both in air ambient for 30 minutes. The geometry of each line was determined using stylus profiler. The correlation between lines resistance and the appropriate geometry enable to obtain a characteristic resistivity from linear regression of plotted values as seen in Figure 6 and Figure 7, respectively. The equation of a relationship between resistivity and resistance was used:

$$R = \rho \frac{l}{A'} + R_0 = \left(\rho \frac{l}{h} \right) \frac{1}{w} + R_0, \quad (3)$$

where R_0 represents residual resistance.



Fig. 5: Ink-jet printed silver lines array of pixelated geometry as 1, 3, 5, 10, 20 and 40 pixels. Length of 71 mm was kept constant

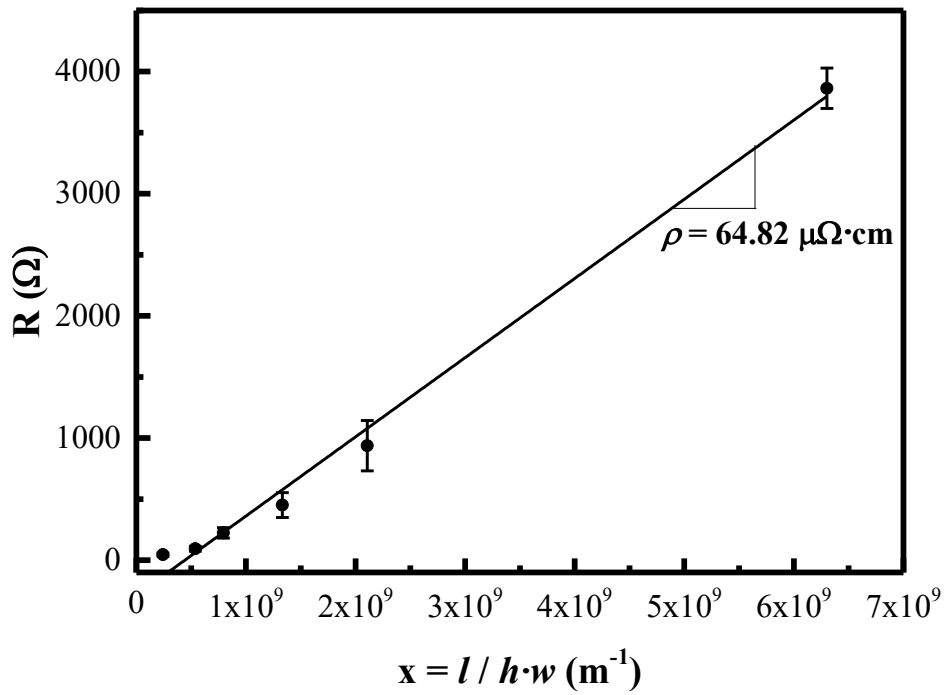


Fig. 6: Linearized dependence of dimensions of pixelated lines on their resistance printed of DGP 40LT-15C ink. Electrical resistivity is extracted from the regression formula

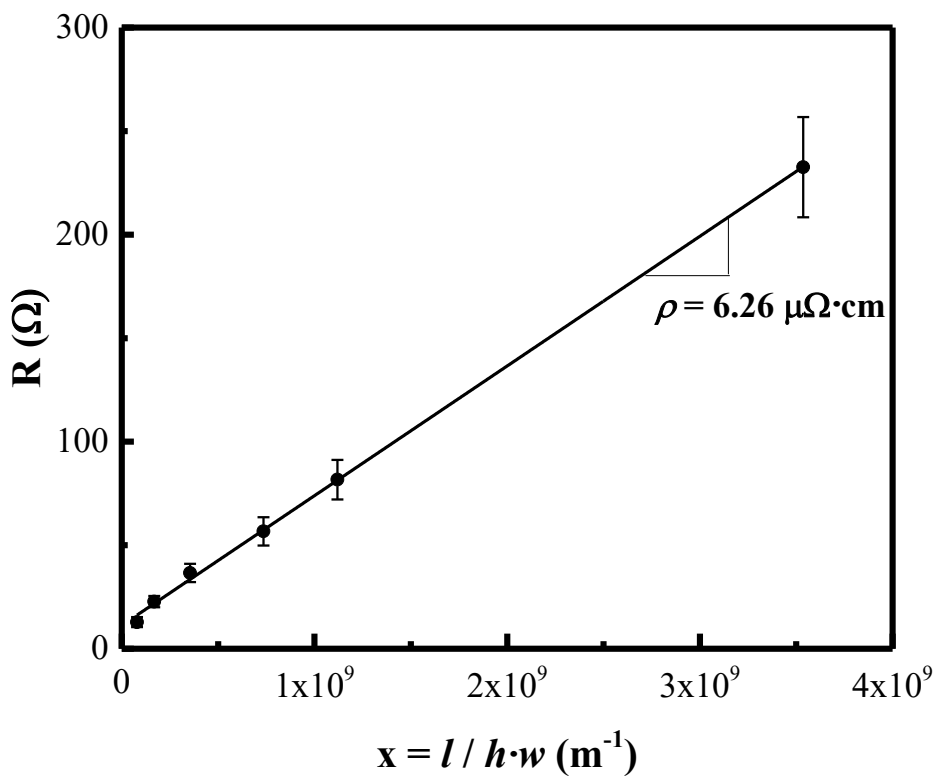


Fig. 7: Linearized dependence of dimensions of pixelated lines on their resistance printed of DGH 55LT-25C ink. Electrical resistivity is extracted from the regression formula

Development of printed conductive structures for electronic devices

Figure 8 illustrates the developing process of a hybrid electronic element containing a printed conductive structure of interconnects and indicating green SMD LEDs. Step 1. involves designing of required structure in an appropriate scale. Subsequently, the image is transferred to the printer pattern creator software, where the resolution parameters are defined. In the next step 2., the structure is printed and its quality is characterized. In the last step 3., the functional components are implemented in the element and connected to a power supply.

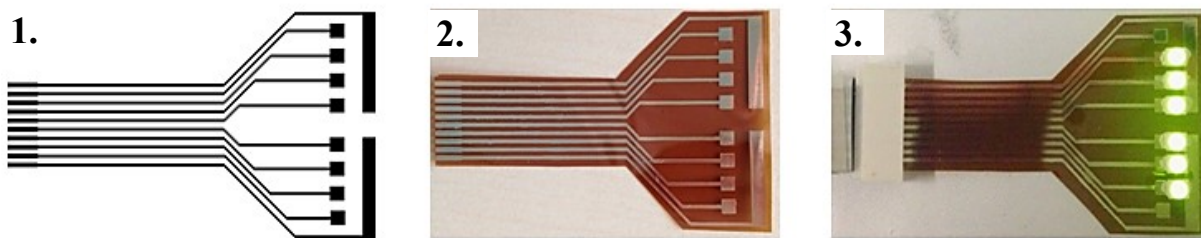


Fig. 8: Development of ink-jet printed device

Conductive interconnects were deposited by ink-jet printing technology from two commercially available silver nanoparticles-based inks on PET and PI foils. Reference samples printed on glass substrate were characterized and resistivity of each material was extracted from linear regression of pixelated lines array measured by using two-point probe method.

The resistivity value of ink DGP 40LT-15C, intended to print on PET foil limited by curing temperature of 150 °C, was determined to 64.8 $\mu\Omega\cdot\text{cm}$. In case of ink DGH 55LT-25C, intended to print on PI foil, the resistivity value was determined to 6.26 $\mu\Omega\cdot\text{cm}$. For comparison, the tabulated resistivity value of pure silver is 1.59 $\mu\Omega\cdot\text{cm}$ (at 20 °C) [47]. The descent of resistivity values of silver inks is given by the solid content and the size of particles. Evaporation of the carrier medium while curing leads to densification and compaction of the structure with diminishing particle size having appropriate bulk density and corresponding residual pore space. While aggregation of particles and formation of conductive channels between them contribute to conductivity, porous space can be assumed to increase the overall resistivity compared to the pure bulk silver.

Indicating SMD LEDs were assembled with printed interconnects and plugged in as a functional flexible circuit. The photograph of a fabricated model sample is seen in Figure 8.

Ink composition development

The original ink composition was experimentally developed within this space of parameters by the trial-error method of changing and alternating always only one variable until a satisfactory performance of the process was achieved. The properties of developed inks with variable nanoparticle loading are listed in Table 1. [4]

Table 1 Main properties of ITO inks, [4]

Nanoparticles loading / wt%	10	15	20	25
Surface tension / $\text{mN}\cdot\text{m}^{-1}$	21.6 \pm 0.1	21.6 \pm 0.1	21.6 \pm 0.1	21.7 \pm 0.1
Density / $\text{kg}\cdot\text{m}^{-3}$	1127.6	1186.7	1241.9	1306.6
Viscosity / $\text{mPa}\cdot\text{s}$	3.078	3.518	4.128	4.703

The optimal amount and ratio of the two additives were determined based on the critical micelle concentration in an aqueous medium. The surface tension was controlled by using a wetting agent which produces a significant decrease in the surface tension of the aqueous system and therefore particularly improves substrate wetting and levelling. The achieved stability of the ink compositions guaranteed their safe use within the timescale of several days is exemplified in Figure 9. [4]

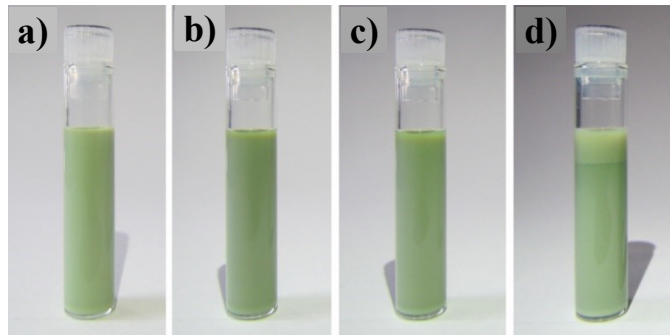


Fig. 9: Demonstrating the achieved stability and the sedimentation progress of the ink composition (25 wt% loading) over time (a) $t = 0$ h, (b) $t = 24$ h, (c) $t = 72$ h, (d) $t = 10$ days. [4]

Dimensionless correlations were used for the analysis of the material-tool-process parameter space according to the literature as described in introductory chapter 4.4. Table 2 summarises the calculated dimensionless criteria of the

prepared inks with the use of optimal ink ejection fluid velocity of $6 \text{ m}\cdot\text{s}^{-1}$ taken into account in this analysis. [4]

Table 2 Calculated dimensionless criteria of prepared inks, [4]

Nanoparticles loading / wt%	10	15	20	25
<i>Re</i>	47.26	43.51	38.81	35.84
<i>We</i>	40.44	42.50	44.42	46.60
<i>Oh</i>	0.13	0.15	0.17	0.19
<i>Z</i>	7.43	6.67	5.82	5.25
<i>Ca</i>	0.86	0.98	1.14	1.30

The graph constructed with the help of the definition of printability boundaries by McKinley and Renardy [34] (originally constructed by Derby [35]) is presented in Figure 10, which shows the field of parameters for stable operations of drop on demand inkjet printing by using logarithmic coordinate system defined by plotting Ohnesorge against Reynolds number. The quadrangle ABCD defines a region, in which the particular fluids are printable and single drop formation may be achieved or merging with the satellite can be expected. [4]

The black full quadrangle in the centre represents the optimum printability space for the Dimatix printer. The characteristic length A is strictly given by the nozzle geometry in the used printing heads and cannot be changed at all.

The changes of the variables involved in the dimensionless criteria result in typical shifts or extensions of this parameter space in the directions indicated by the six arrows marked from **a** to **f**. Decreasing the fluid velocity corresponds to the direction **a** while the use of higher velocity shifts the area in the direction **d**. Increasing the surface tension shifts the parameter space border downwards in direction **f** while decreasing the surface tension results in the shift upwards in direction **c**. Increasing the fluid viscosity results in the shift along the arrow **b** and decreasing the viscosity extends the area in the direction of the arrow **e**. Although a good printability was finally achieved for all compositions by varying the parameters, the point closest to the centre of the printability area corresponds to the ink composition with 25 wt% of ITO.

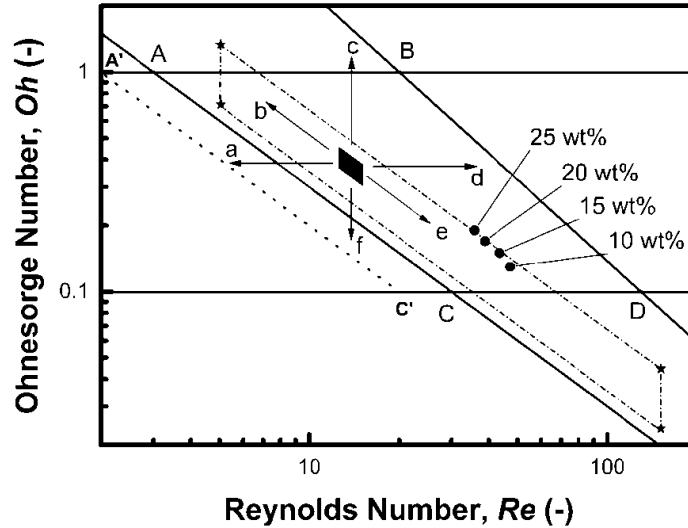


Fig. 10: Map of Oh and Re dimensionless correlations space for a printing process with the printability area $ABCD$ replotted according to McKinley and Renardy [34]. For a detailed description please see text. [4]

Among the single criterion approaches, the importance of the Weber number was used and raised again. On the other hand, the description of the processing window requires at least a two-dimensional map. We refrained from incorporating the viscoelasticity into our models in favour of reemploying older yet still valuable models limited for Newtonian fluids only. The presented approach enables fast advances in ink formulations and process development with the used DOD printer and simple experimental instrumentation.

Gas sensing test

Prepared sensing devices consisting of ink-jet deposited ITO films from 25 wt% loading ink were arranged as schematically shown in Figure 11.

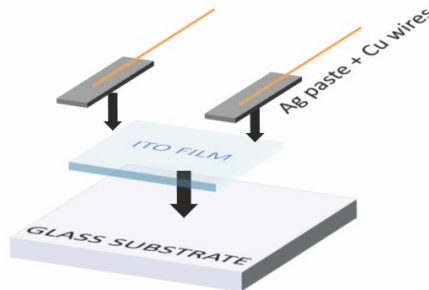


Fig. 11: Schematic design of sensing device, [4]

A variation in the electrical resistance of the printed sensors upon exposure to saturated vapours of toluene in ambient air (toluene/air) at 25 °C was noticed as

shown in Figure 12 (upper graph window). In air atmospheres, even the low-temperature sensing mechanism can be explained by well-established models for n-type semiconductors. Among them, the oxygen vacancy model (reduction-reoxidation mechanism) seems to be the most favourable. Baseline drift can be attributed to the presence of coexisting gases in an uncontrolled ambient laboratory atmosphere since experienced regardless of the pre-equilibration of the sensor. Because of the porous nature of the layer, as well as a low operating temperature, the sensor requires a longer recovery time needed for desorption and diffusion of vapour molecules from the porous film.

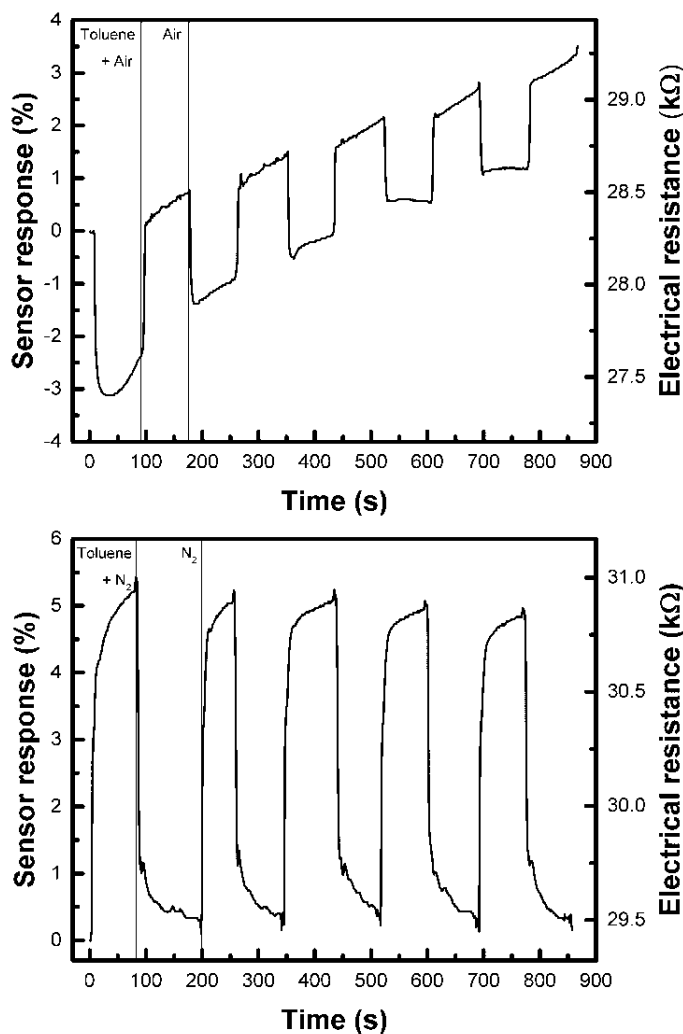


Fig. 12: The sensor's response magnitude to the exposure of Toluene/Air and the saturated vapours of Toluene in an N₂ ambient atmosphere at 25 °C. [4]

An increase of resistance when the sensor is exposed to saturated toluene vapours in an oxygen-free atmosphere as shown in Figure 12 (lower graph window) was observed. This conductivity behaviour inversion can be attributed

to a change to the sensing mechanism after placing the sensor into an N_2 atmosphere similarly as in [45,48-50]. Despite relatively small overall sensitivity, fast response and recovery times to toluene vapours at laboratory temperature were observed and the overall sensitivity of the device was slightly larger and the sensor response was more stable over the tested number of cycles in pure nitrogen than in open air ambient.

Printing and hydrothermal growth of nanostructures

The nanoseed precursor was ink-jet deposited onto pre-printed interdigitated silver electrode structures from the prepared solution which was subsequently subjected to hydrothermal growth for 24 hours at 92 °C at three different concentrations of a growth-direct agent resulting in different thickness, shape and growth direction of nanostructures as seen in Figure 13. To note, a further increase of PEI concentration did not yield any defined structure. Grown ZnO nanostructures were subsequently dried and observed by electron microscopy.

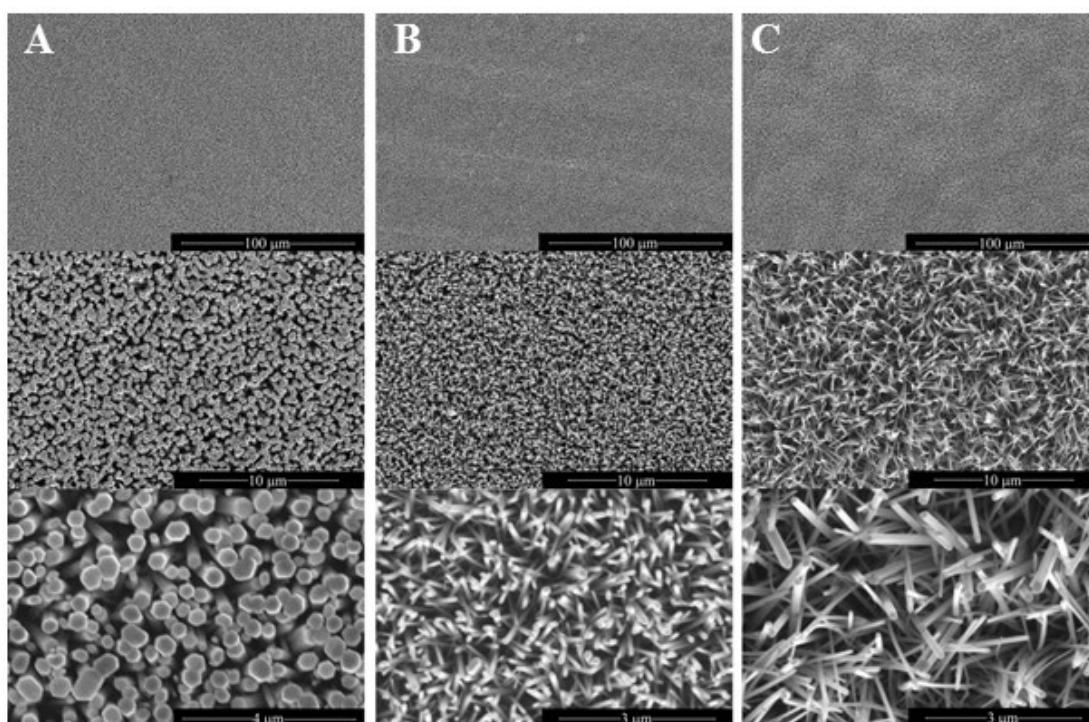


Fig. 13: SEM pictures display homogeneity of nanostructures, as well as detailed shapes of nanowires at different magnitudes. Nanostructures in column a) were grown in bath without addition of growth-direct agent, bath in column b) contained 0.008 M and column c) 0.016 M solution of growth-direct agent.

Development of flexible gas sensor of ZnO nanostructures

While in the previously described in this thesis, parallel conductive pads were employed as contact electrodes of the resistive layer (schematically illustrated in Figure 11), capacitive planar geometry of conducting electrodes called interdigitated electrodes (IDE) was designed and tested in this section. This electrode configuration is the most commonly utilized design allowing the detection of resistance or capacitance of sensitive layer generating output signal associated with the exposed gas. Thus, the conductivity of the sensitive material and the distance of the electrodes in between the material is placed, determine the initial signal value which must be chosen within the range of the measuring instrument. The proprietary design of the device is schematically illustrated in Figure 14. The sensing responses of prepared devices were tested for the presence of ethanol at room temperature and the responses of the variously formed nanostructures were compared.

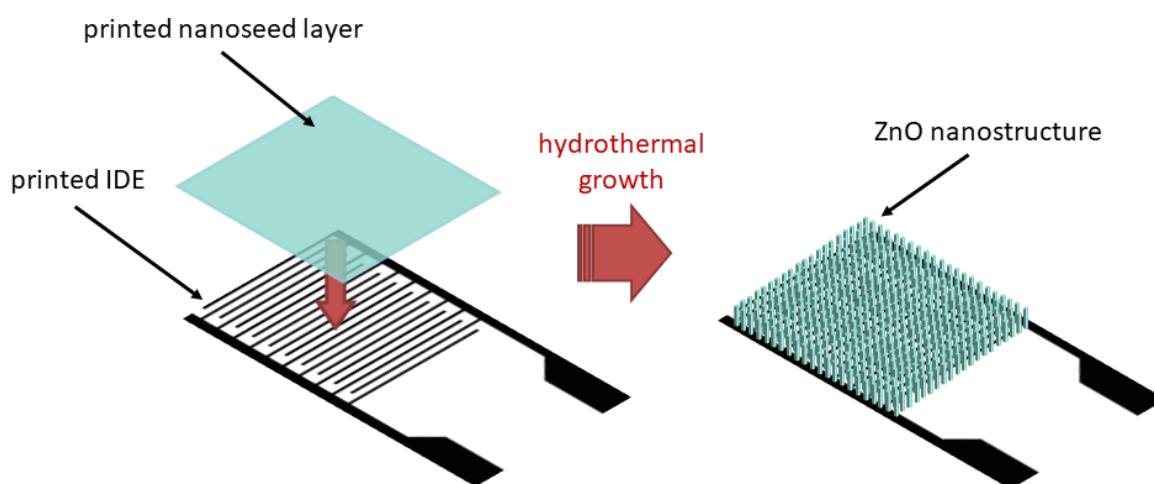


Fig. 14: Schematic illustration of fabrication process of flexible sensing device

Gas sensing test

Three different methods of hydrothermal ZnO nanowire growth were applied, thus three sets of flexible specimens were obtained and tested at the room temperature in the apparatus schematically described in Figure 4. The three types of response curves to the pulses of the analyte in dry air flow (200 sccm, dose of 1 μ l of ethanol injected and instantaneously vaporised every 5 minutes, performed in dark) are plotted in the graph in Figure 15. The first type of nanostructured ZnO which consists of thick well-ordered vertically aligned nanorods does not exhibit

any response to the pulses at all. Moreover, a continuous and non-monotonous drift of the baseline was observed although the conditions of the carrier gas were under perfect control by using synthetic gas of high purity from a gas cylinder. Thus no repeatability can be expected for this type of device (material) and it was excluded from further considerations. Application of the PEI growth modifying agent allowed to prepare thinner nanowires in the form of a forest. Use of 0.008 mM concentration of PEI in the growing bath solution resulted into an ordered but vertically slightly misaligned structure while doubling the concentration of PEI (16 mM) resulted into even more misaligned nanowire structure with longer but thicker wires having apparently more connections than in the previous case. Influence of such morphology is manifested in the response curves for these devices which are plotted in Figure 32, as well. The 8 mM sample has a bigger response to each pulse than the 16 mM sample which can be correlated with the thickness of the nanowires. The thinner the nanowires the bigger sensitivity can be expected. On the other hand, the stability of the baseline and background signal (i.e. off state) was much better for the last type on nanostructure, possibly due to better development of nanowire percolation.

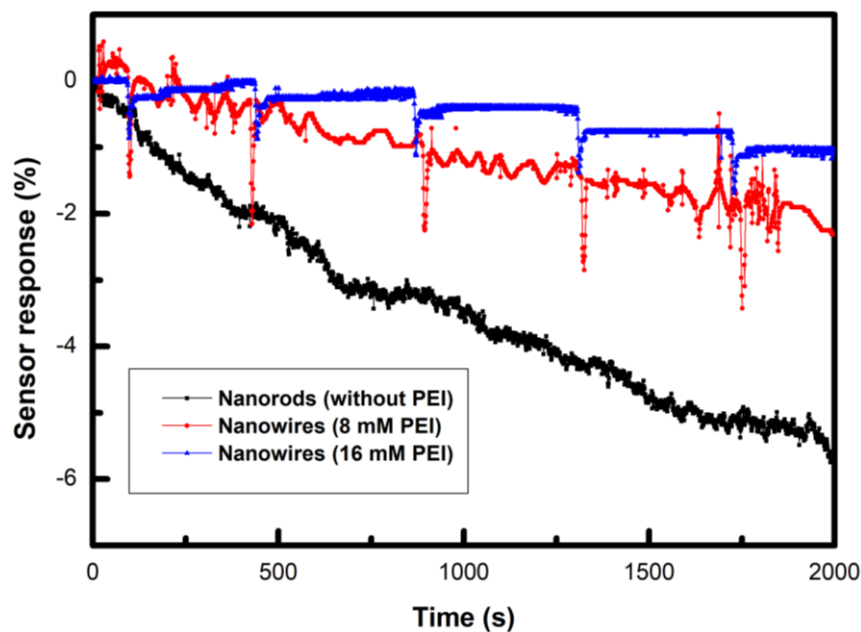


Fig. 15: The response magnitudes of sensing devices consisting of ZnO nanostructures formed at various concentrations of growth-direct agent to the exposure of pulses of Ethanol in dried Air at 25 °C

Development of UV-assisted gas sensor of ZnO nanowire network

On the base of findings previously observed, the last type of material (sensing structure) was selected for further development of a novel integrated UV-assisted low temperature gas sensing device intended to integrate directly on top of the UV irradiation source (quartz window of the LED emitting at $\lambda = 365$ nm) while in the literature, the sensor was always irradiated from the top by an external UV light source. The closest contact between the semiconducting ZnO sensing material and the source window is achieved by utilization of this design, however, such geometry imposes strong requirements on the active layer thickness (fineness of the structure) and fabrication process development. Figure 16 depicts the sequence of the three fabrication steps including (i) printing of all the miniature motifs on the UV LED window followed by (ii) hydrothermal growth requiring protection of the LED substrate against corrosion by the chemical growth bath solution and accomplished by (iii) assembly of the SMD to the printed conductive platform for operation of the whole device.

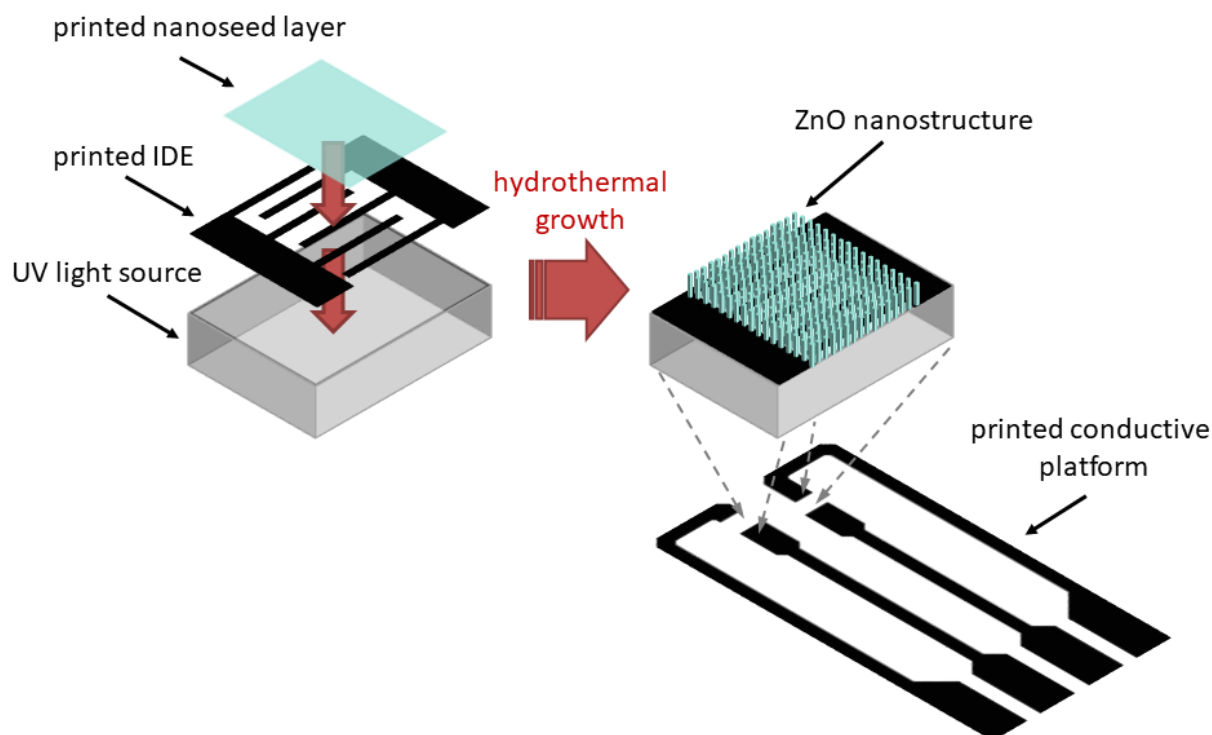


Fig. 16: Schematic illustration of fabrication process of integrated sensing element assembled on printed circuit board

Gas sensing test

Prepared sensing device was tested in the same apparatus as the flexible IDE devices at the room temperature, however, the flow rate of the carrier gas (synthetic air) was 200 sccm and amount of 1 μl of ethanol was injected and instantaneously vaporised every 2 minutes. Response curves to these analyte pulses were recorded with and without UV activation. The results are plotted in Figure 36. Forward voltage for the used LED was 3.6 V, which is the optimum performance as suggested by the producer of the diode. It can be clearly seen in the graph that the application of UV enhances the response of the sensing element and increases apparently the recovery time. Since the initial resistance value reaches an order of $\text{k}\Omega$, a sharp decrease of about one order of magnitude after UV activation was experienced. Therefore, two plausible explanations can be considered that it is due to the sensitivity increase and saturation of the system at the peak (pulse) arrival time or due to modified dynamics of the recovery process. Nevertheless, the baseline (background in off-state) stability and reproducibility seem to be sufficient for both regimes of the device operation. With the full awareness of the need of other characterizations remaining to be performed in future work, it can be concluded that the main achievement of the proof of concept device and demonstration of the original device functionality was accomplished.

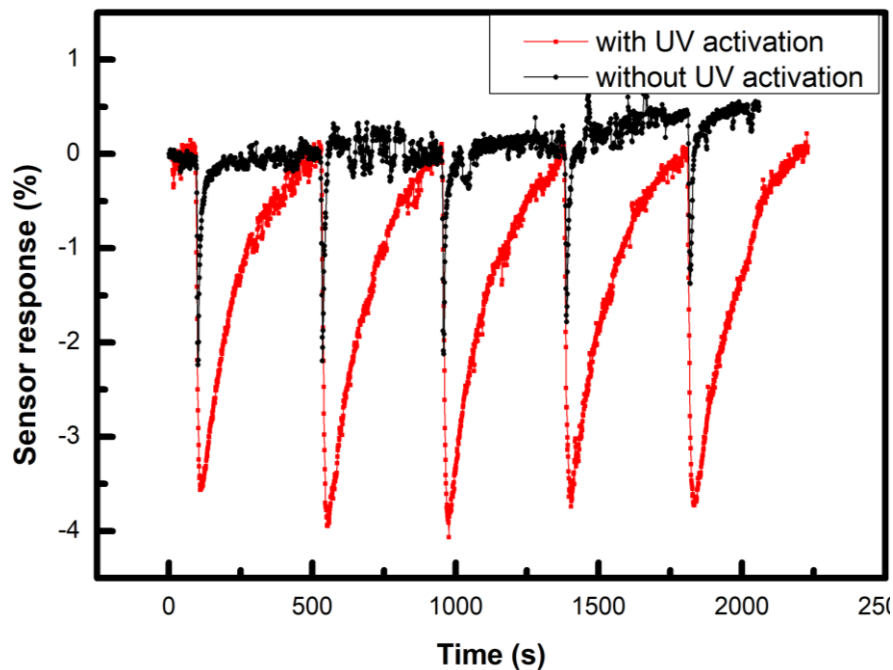


Fig. 17: The response magnitudes of integrated sensing device consisting of ZnO nanowire network to the exposure of pulses of Ethanol in dried Air at 25 °C in dark gas chamber and with activated UV-LED

9. SUMMARY OF CONTRIBUTIONS TO SCIENCE AND PRAXIS

An original method of preparation of sensors for toluene and ethanol as representative volatile organic compounds were developed by using material ink-jet printing technique from both originally prepared and commercially available nanoparticles-based and solution-based inks. These sensor devices were prepared by a low-temperature process enabling the use of polymer components and successfully demonstrated their function when operated at the room temperature. Towards these ends, structure, morphology and properties of deposited materials and prepared devices were investigated with respect to their function. It was revealed, that the sensing mechanism of the n-type semiconductors still remains in action although its effectivity is quite low at the room temperature. Moisture and other components of ambient atmosphere interfere with the sensor function of the device by non-specific stimulation of its response resulting thus into inevitable shifts of the measurement baseline (off-state background) of the device. This disadvantage is normally overcome by the operation of the sensor at high temperature, but addressing this issue at the room temperature was one of the goals of this theses. Indeed, a miniature device prepared directly on the quartz window of a UV LED was developed and successfully fabricated to demonstrate the viability of the use of UV cold activation of the semiconducting active sensor layer instead of the utilization of high temperature.

The research work presented in this thesis can be considered an original contribution to unlocking the future improvement of sensitivity of metal oxide based sensors to detect organic vapours and gases at room operating temperatures. To summarize the contribution of the results corresponding to objectives defined in the aim of the doctoral thesis, following practical points, as well as theoretical contributions can be emphasized:

- Optimization of the preparation of conductive interconnects and electrodes by the ink-jet printing using silver nanoparticles-based inks on polymer foils applicable in flexible electronics.
- Development of ink based on ITO nanoparticles and its deposition by the ink-jet printing technique on a suitable substrate. A framework using dimensionless criteria was developed for ink formulation and printing process optimization. Fabrication of a toluene sensing device which can be operated at the room temperature was demonstrated.

- The sensing mechanism of the ITO sensor at low temperature was elucidated as the typical response for an n-type semiconductor. The low efficiency and inevitable interference of the ambient atmosphere stimulated the next research on ZnO based sensors, where the cold UV activation instead high-temperature operation was expected plausible.
- A combination of printing and hydrothermal growth resulted into the preparation of an IDE designed sensor fabricated on a polymer substrate which allowed to find a suitable morphology of ZnO nanowire forest and method of its preparation which was successfully used in the fabrication of a novel integrated UV-assisted low temperature operated gas sensing device.

REFERENCES

- [1] H. Kipphan, Handbook of Print Media: Technologies and Production Methods, (2001) 1207.
- [2] Hutchings, Ian M., Martin, Graham, Inkjet technology for digital fabrication, (2012) 390.
- [3] Anonymous, FUJIFILM Dimatix Materials Printer DMP-2800 Series User Manual ed. U.S.A.: FUJIFILM Dimatix, Inc. (2010).
- [4] J. Maslik, I. Kuritka, P. Urbanek, P. Krcmar, P. Suly, M. Masar, M. Machovsky, Water-Based Indium Tin Oxide Nanoparticle Ink for Printed Toluene Vapours Sensor Operating at Room Temperature, Sensors. 18 (2018).
- [5] J. Jeong, J. Lee, H. Kim, H. Kim, S. Na, Ink-jet printed transparent electrode using nano-size indium tin oxide particles for organic photovoltaics, Solar Energy Mater. Solar Cells. 94 (2010) 1840-1844.
- [6] S. Magdassi, The Chemistry of Inkjet Inks, First ed., World Scientific Publishing Co. Pte. Ltd., Singapore, 2010.
- [7] R.H. Leach, The Printing Ink Manual, Kluwer, Dordrecht, 1999.
- [8] H. Mbarek, M. Saadoun, B. Bessaïs, Screen-printed Tin-doped indium oxide (ITO) films for NH₃ gas sensing, Materials Science and Engineering: C. 26 (2006) 500-504.
- [9] B. Bessaïs, N. Mliki, R. Bennaceur, Technological, structural and morphological aspects of screen-printed ITO used in ITO/Si type structure, Semiconductor Science and Technology. 8 (1993) 116-121.
- [10] V.S. Vaishnav, S.G. Patel, J.N. Panchal, Development of indium tin oxide thin film toluene sensor, Sensors Actuators B: Chem. 210 (2015) 165-172.
- [11] M. Afshar, E.M. Preiß, T. Sauerwald, M. Rodner, D. Feili, M. Straub, K. König, A. Schütze, H. Seidel, Indium-tin-oxide single-nanowire gas sensor fabricated via laser writing and subsequent etching, Sensors Actuators B: Chem. 215 (2015) 525-535.
- [12] C. Lin, H. Chen, T. Chen, C. Huang, C. Hsu, R. Liu, W. Liu, On an indium-tin-oxide thin film based ammonia gas sensor, Sensors Actuators B: Chem. 160 (2011) 1481-1484.

- [13] A. Facchetti, T.J. Marks, *Transparent Electronics: From Synthesis to Applications*, in: *Anonymous Transparent Electronics: From Synthesis to Applications*, , 2010.
- [14] S.D. Hoat, *Fundamentals of inkjet printing : the science of inkjet and droplets*, (2016) 449.
- [15] J. Korvink G., P. Smith J., D. Shin, *Inkjet-based micromanufacturing*, (2012) 371.
- [16] O.A. Basaran, H. Gao, P.P. Bhat, *Nonstandard Inkjets*, *Annu. Rev. Fluid Mech.* 45 (2013) 85-113.
- [17] J.R. Castrejon-Pita, W.R.S. Baxter, J. Morgan, S. Temple, G.D. Martin, I.M. Hutchings, *Future, opportunities and challenges of inkjet technologies, Atomization and Sprays.* 23 (2013) 541-565.
- [18] O.A. Basaran, *Small-scale free surface flows with breakup: Drop formation and emerging applications*, *AIChE J.* 48 (2004) 1842-1848.
- [19] J. Heinzl, C.H. Hertz, *Ink-Jet Printing*, *Advances in Electronics and Electron Physics.* 65 (1985) 91-171.
- [20] E.P. Furlani, B.G. Price, G. Hawkins, A.G. Lopez, *Thermally induced Marangoni instability of liquid micro-jets with application to continuous inkjet printing*, (2006) 534-537.
- [21] E.P. Furlani, *Numerical analysis of nonlinear deformation and breakup of slender microjets with application to continuous inkjet printing*, (2007) 444-446.
- [22] E.P. Furlani, *Temporal instability of viscous liquid microjets with spatially varying surface tension*, *Journal of Physics A: Mathematical and General.* 38 (2005) 263.
- [23] E. Furlani, *Thermal modulation and instability of Newtonian liquid microjets*, (2005) 668-671.
- [24] E.P. Furlani, M.S. Hanchak, *Nonlinear analysis of the deformation and breakup of viscous microjets using the method of lines*, *Int. J. Numer. Meth. Fluids.* 65 (2011) 563-577.
- [25] H. Wijshoff, *The dynamics of the piezo inkjet printhead operation*, *Physics Reports.* 491 (2010) 77-177.

- [26] H. Wu, W. Hwang, H. Lin, Development of a three-dimensional simulation system for micro-inkjet and its experimental verification, *Materials Science & Engineering A*. 373 (2004) 268-278.
- [27] T.W. Shield, D.B. Bogy, F.E. Talke, Drop formation by DOD ink-jet nozzles: A comparison of experiment and numerical simulation, *IBM Journal of Research and Development*. 31 (1987) 96-110.
- [28] F. Tseng, C. Kim, C. Ho, A high-resolution high-frequency monolithic top-shooting microinjector free of satellite drops - Part II: Fabrication, implementation, and characterization, 11 (2002) 437.
- [29] T. Lindemann, D. Sassano, A. Bellone, R. Zengerle, P. Koltay, I. Olvetti, Three-dimensional CFD-simulation of a thermal bubble jet printhead, (2004) 227-230.
- [30] N. Yamazoe, G. Sakai, K. Shimano, Oxide semiconductor gas sensors, *Catalysis Surveys from Asia*. 7 (2003) 63-75.
- [31] G. Cummins, Marc P.Y. Desmulliez, Inkjet printing of conductive materials: a review, *Circuit World*. 38 (2012) 193-213.
- [32] J.A. Roberson, J.J. Cassidy, H.M. Chaudhry, *Hydraulic Engineering*, Wiley, 1998.
- [33] E. Kim, J. Baek, Numerical study on the effects of non-dimensional parameters on drop-on-demand droplet formation dynamics and printability range in the up-scaled model, *Phys. Fluids*. 24 (2012) 082103.
- [34] G.H. McKinley, M. Renardy, Wolfgang von Ohnesorge, *Phys. Fluids*. 23 (2011) 127101.
- [35] B. Derby, Inkjet Printing of Functional and Structural Materials: Fluid Property Requirements, Feature Stability, and Resolution, *Annu. Rev. Mater. Res.* 40 (2010) 395-414.
- [36] H.A. Andersson, A. Manuilskiy, S. Haller, M. Hummelgård, J. Sidén, C. Hummelgård, H. Olin, H. Nilsson, Assembling surface mounted components on ink-jet printed double sided paper circuit board, *Nanotechnology*. 25 (2014) 094002.
- [37] T. Joubert, P.H. Bezuidenhout, H. Chen, S. Smith, K.J. Land, Inkjet-printed Silver Tracks on Different Paper Substrates, *Materials Today: Proceedings*. 2 (2015) 3891-3900.

- [38] T. Ohlund, A. Schuppert, B. Andres, H. Andersson, S. Forsberg, W. Schmidt, H. Nilsson, M. Andersson, R. Zhang, H. Olin, Assisted sintering of silver nanoparticle inkjet ink on paper with active coatings, *RSC Adv.* 5 (2015) 64841-64849.
- [39] W. Shen, X. Zhang, Q. Huang, Q. Xu, W. Song, Preparation of solid silver nanoparticles for inkjet printed flexible electronics with high conductivity, *Nanoscale.* 6 (2014) 1622-1628.
- [40] J. Matyas, P. Slobodian, L. Munster, R. Olejnik, P. Urbanek, Microstrip antenna from silver nanoparticles printed on a flexible polymer substrate, *Materials Today: Proceedings.* 4 (2017) 5030-5038.
- [41] J. Fraden, *Handbook of Modern Sensors: Physics, Designs, and Applications*, Springer-Verlag, New York, 2010.
- [42] K. Kalantar-zadeh, *Sensors: An Introductory Course*, Springer US, New York, 2013.
- [43] J.S. Wilson, *Sensor Technology Handbook*, Newnes, Burlington, 2005.
- [44] J. Janata, *Principles of Chemical Sensors*, Springer US, New York, 2009.
- [45] M.A. Carpenter, S. Mathur, A. Kolmakov, *Metal Oxide Nanomaterials for Chemical Sensors*, Springer, New York Hiedelberg Dordrecht London, 2013.
- [46] G. Korotcenkov, *Handbook of Gas Sensor Materials: Properties, Advantages and Shortcomings for Applications Volume 1: Conventional Approaches*, 1st ed., Springer-Verlag New York, 2013.
- [47] Smithsonian Institution., W.E. Forsythe, *Smithsonian Physical Tables*, 9th edition ed., The Institution, Washington, D.C., 1954.
- [48] D. Smyth, The Role of Impurities in Insulating Transition-Metal Oxides, *Progress in Solid State Chemistry.* 15 (1984) 145-171.
- [49] D. Williams, P. Moseley, Dopant Effects on the Response of Gas-Sensitive Resistors Utilizing Semiconducting Oxides, *Journal of Materials Chemistry.* 1 (1991) 809-814.
- [50] A. Gurlo, N. Barsan, A. Oprea, M. Sahm, T. Sahm, U. Weimar, An n- to p-type conductivity transition induced by oxygen adsorption on alpha-Fe₂O₃, *Appl. Phys. Lett.* 85 (2004) 2280-2282.

LIST OF FIGURES

<i>Figure 1 – Thin film formation using material ink-jet printer. Adopted from [31]</i>	3
<i>Figure 2 – Ink components and requirements</i>	5
<i>Figure 3 – Ink suitability using dimensionless criteria, Adopted from [34]</i>	8
<i>Figure 4 – Schematic illustration of gas sensing measurement setup</i>	13
<i>where R_0 represents residual resistance</i>	14
<i>Figure 8 – Development of ink-jet printed device</i>	16
<i>Figure 13 – SEM pictures display homogeneity of nanostructures, as well as detailed shapes of nanowires at different magnitudes. Nanostructures in column a) were grown in bath without addition of growth-direct agent, bath in column b) contained 0.008 M and column c) 0.016 M solution of growth-direct agent.</i>	21
<i>Figure 14 – Schematic illustration of fabrication process of flexible sensing device</i>	22
<i>Figure 15 – The response magnitudes of sensing devices consisting of ZnO nanostructures formed at various concentrations of growth-direct agent to the exposure of pulses of Ethanol in dried Air at 25 °C</i>	23
<i>Figure 16 – Schematic illustration of fabrication process of integrated sensing element assembled on printed circuit board</i>	24
<i>Figure 17 – The response magnitudes of integrated sensing device consisting of ZnO nanowire network to the exposure of pulses of Ethanol in dried Air at 25 °C in dark gas chamber and with activated UV-LED</i>	25

LIST OF TABLES

<i>Table 1 – Main properties of ITO inks</i>	17
<i>Table 2 – Calculated dimensionless criteria of prepared inks</i>	18

LIST OF ABBREVIATIONS

Alphabetically ordered

CIJ	Continuous ink-jet
CMC	Critical micelle concentration
DOD	Drop-on-demand
ITO	Indium tin oxide
LED	Light-emitting diode
MFC	Mass flow controller
NPs	Nanoparticles
PEI	Polyethyleneimine
PET	Polyethylene terephthalate
PI	Polyimide
PTFE	Polytetrafluoroethylene
PZT	Lead zirconium titanate
RFID	Radio frequency identification
SMD	Surface-mount device
UV	Ultraviolet

LIST OF SYMBOLS

Alphabetically ordered

A	Characteristic length
h	Conductor thickness
l	Conductor length
λ	Wavelength
O	Wetted perimeter
R	Electrical resistance
R_0	Residual resistance
R_{air}	Sensor resistance in air atmosphere
R_{gas}	Sensor resistance upon vapours ambience
ρ	Density
S	Area
S_R	Sensor response ratio
w	Conductor width

LIST OF DIMENSIONLESS NUMBERS

Alphabetically ordered

<i>Ca</i>	Capillary number
<i>La</i>	Laplace number
<i>Oh</i>	Ohnesorge number
<i>Re</i>	Reynolds number
<i>We</i>	Weber number
<i>Z</i>	Z number, Reciprocal Ohnesorge number

LIST OF UNITS

Alphabetically ordered

A	Characteristic length
h	Conductor thickness
l	Conductor length
λ	Wavelength
O	Wetted perimeter
R	Electrical resistance
R_0	Residual resistance
R_{air}	Sensor resistance in air atmosphere
R_{gas}	Sensor resistance upon vapours ambience
ρ	Density
S	Area
S_R	Sensor response ratio
w	Conductor width

LIST OF PUBLICATIONS

1. RAFAJOVÁ, M.; MINAŘÍK, A.; SMOLKA, P.; MRÁČEK, A.; MAŠLÍK, J.; MACHOVSKÝ, M. Factors determining hydrophobicity silicon-based materials. *Chemické Listy*. 2014, **108**(1), 35-39. ISSN: 1213-7103
2. ŠULY, P.; KRČMÁŘ, MAŠLÍK, J.; URBÁNEK, P.; KUŘITKA, I. Poly(vinyl alcohol): formulation of a polymer ink for the patterning of substrates with a drop-on-demand inkjet printer. *Materiali in tehnologije*. 2017, **51**(1), 41-48. ISSN: 1580-2949. doi: 10.17222/mit.2015.180
3. TORRES-CANAS, F.; BLANC, CH.; MAŠLÍK, J.; TAHIR, S.; IZARD, N.; KARASAHIN, S.; CASTELLANI, M.; DAMMASCH, M.; ZAMORA-LEDEZMA, C.; ANGLARET, E. Morphology and anisotropy of thin conductive inkjet printed lines of single-walled carbon nanotubes. *Materials Research Express*. 2017, **4**(3). ISSN: 2053-1591
4. KRČMÁŘ, P.; KUŘITKA, I.; MAŠLÍK, J.; URBÁNEK, P.; BAŽANT, P.; MACHOVSKÝ, M.; ŠULY, P.; MĚRKA, P. The preparation and characterization of CuO inkjet inks for fully printed alcohol vapours and humidity sensors on flexible polymer substrate. *Sensors*. 2018 – Submitted
5. MASLÍK, J.; KURITKA, I.; URBANEK, P.; KRČMAR, P.; ŠULY, P.; MASAR, M. and MACHOVSKY, M. Water-Based Indium Tin Oxide Nanoparticle Ink for Printed Toluene Vapours Sensor Operating at Room Temperature. *Sensors*. 2018, **18**(10)
6. ANDERSSON, H.; ŠULY, P.; THUNGSTRÖM, G.; ENGHOLM, M.; ZHANG, R.; MAŠLÍK, J.; OLIN, H. PEDOT: PSS Thermoelectric Generators Printed on Paper Substrates. *J. Low Power Electron. Appl.* 2019, **9**(14)

Utility models and patent

1. MINAŘÍK, A.; SMOLKA, P.; MRÁČEK, A.; NOVÁK, L.; MINAŘÍK, M.; MAŠLÍK, J. Variable multiposition injection pump. ID 22866 – Utility model
2. MINAŘÍK, A.; SMOLKA, P.; NOVÁK, L.; MINAŘÍK, M.; MAŠLÍK, J. Experimental device for modification of polymorphic morphology in non-stationary temperature fields. ID 23263 – Utility model

3. KUŘITKA, I.; URBÁNEK, P.; KRČMÁŘ, P.; MAŠLÍK, J. Polymeric Ink for Material Printing. ID 26729 – Utility model
4. KUŘITKA, I.; URBÁNEK, P.; KRČMÁŘ, P.; MAŠLÍK, J.; ŠULY, P. Inorganic ink based on nanoparticles, intended especially for material printing. ID 307435 – Patent

Conference contributions

1. KRČMÁŘ, P.; URBÁNEK, P.; KUŘITKA, I.; MAŠLÍK, J.; BARTOŠ J. The Effect of the Exalite on Photoluminescence of Poly(methylphenylsilane) in Thin Films, In *NANOCON Conference proceedings*. 2012, Brno, Czech Republic. ISBN 978-80-87294-32-1
2. URBÁNEK, P.; KUŘITKA, I.; KRČMÁŘ, P.; MAŠLÍK, J.; BARTOŠ J. Polysilanes Thin Films Doped by Coumarin, In *NANOCON Conference proceedings*. 2012, Brno, Czech Republic. ISBN 978-80-87294-32-1
3. MAŠLÍK, J.; URBÁNEK, P.; KUŘITKA, I.; KRČMÁŘ, P. Paper No P20: Surface Modification of ITO-Coated PET Foil for Material Printing. In: *SID Symposium Digest of Technical Papers, 70-71. EuroDisplay 2013*, London, United Kingdom. doi: 10.1002/sdtp.33
4. URBÁNEK, P.; KUŘITKA, I.; KRČMÁŘ, P.; MAŠLÍK, J. Paper No P31: Optoelectronic Properties of MEH-PPV Thin Films Influenced by their Thickness. In: *SID Symposium Digest of Technical Papers, 105–107. EuroDisplay 2013*, London, United Kingdom. doi: 10.1002/sdtp.32
5. URBÁNEK, P.; ŠEVČÍK, J.; MAŠLÍK, J.; KRČMÁŘ, P.; KUŘITKA, I.; ŠULY, P.; HANULÍKOVÁ, B. The influence of ZnO nanoparticles content on the luminescence of the MEH-PPV in OLED devices. In: *Plastko 2014 Conference Proceedings*, Zlín, Czech Republic. ISBN 978-80-7454-335-7
6. ŠULY, P.; KRČMÁŘ, P.; MAŠLÍK, J.; URBÁNEK, P.; KUŘITKA, I. Polyvinyl Alcohol: Preparation of a Polymer Ink for Patterning of Substrates by Piezoelectric Drop-on-demand Inkjet Printer. In: *23rd ICMT Conference*. 2015, Portorož, Slovenia
7. MAŠLÍK, J.; KUŘITKA, I.; URBÁNEK, P.; KRČMÁŘ, P.; ŠULY, P.; MUNSTER, L. Water-based Indium Tin Oxide Nanoparticles Ink for Printed Ammonia Gas Sensor. In *Sustainable Science Materials and Technology*. 2015, Paris, France

8. ŠEVČÍK, J.; URBÁNEK, P.; ŠULY, P.; URBÁNEK, M.; MAŠLÍK, J.; ANTOŠ, J.; KUŘITKA, I. Enhanced electrical and optical properties of organic light emitting devices. In: *Plastko 2016 Conference Proceedings*, Zlín, Czech Republic. ISBN 978-80-7454-590-0
9. FORSBERG, V.; MAŠLÍK, J.; ANDERSSON, H.; HUMMELGÅRD, M.; TOIVAKKA, M.; KOPPOLU, R.; DAHLSTRÖM, Ch.; OLIN, H.; NORGRÉN, M. Printability of functional inkjet inks onto commercial inkjet substrates and a taylor-made pigment-coated paper. Presented at the *E-MRS, European Materials Research Society Spring Meeting 2018*, 2018, Strasbourg, France
10. MAŠLÍK, J.; ANDERSSON, H.; FORSBERG, V.; ENGHOLM, M.; ZHANG, R.; OLIN, H. Temperature sensor based on PEDOT: PSS ink-jet printed on paper substrate. Presented at the *20th International Workshop on Radiation Imaging Detectors*, 2018, Sundsvall, Sweden

Pedagogic activities

Participated on teaching in laboratory classes of “Preparation and Characterization Methods” and “Nanomaterials and Nanotechnology”

Trainings

Scanning probe microscopy course, Czech Metrology Institute (Brno, Czech Republic)

CURRICULUM VITAE

Personal information

Name: Jan Mašlík
Date of birth: 15th October 1987
Place of birth: Zlín, Czech Republic

Affiliation: Polymer Centre, Faculty of Technology, Tomas Bata University in Zlin, Namesti T.G. Masaryka 275, 76272 Zlin, Czech Republic

E-mail: maslik@utb.cz; jan.maslik@angstrom.uu.se

Education

2013 – 2019

Tomas Bata University in Zlin, Faculty of Technology, Ph.D. studies in Chemistry and Materials Technology, Specialization: Technology of Macromolecular Compounds

2011 – 2013

Tomas Bata University in Zlin, Faculty of Technology, Master's degree in Chemistry and Materials Technology, Specialization: Material Engineering

2008 – 2011

Tomas Bata University in Zlin, Faculty of Technology, Bachelor's degree in Chemistry and Materials Technology, Specialization: Material Engineering

2004 – 2008

Technical High School Otrokovice

Work experience

2019/02 – to date

Department of Engineering Sciences, Division of
Microsystems Technology, Ångström Laboratory,
Uppsala University, Lagerhyddsvägen 1,
752 37 Uppsala, Sweden
Research assistant

2015 – 2019

Centre of Polymer Systems, Tomas Bata University in Zlín,
Trida Tomase Bati 5678, 760 01 Zlín, Czech Republic
Project researcher

Stays abroad

2017/09 – 2017/11

ERASMUS+ Traineeship at Department of Electronics
Design, Mid Sweden University, Holmgatan 10, 85170
Sundsvall, Sweden

2015/10 – 2016/01

ERASMUS+ Study Stay at Laboratoire Charles Coulomb,
Université de Montpellier, Batiment 13, 34095
Montpellier, France

Projects

Internal funding

IGA/FT/2012/025 – Modified polymer materials for thin films – member of the research team

IGA/FT/2013/025 – Material printing of polymer and inorganic inks for advanced applications – member of the research team

IGA/FT/2014/006 – Modification of polymer substrates and new materials for inkjet printing of sensors – project investigator (head of research team)

IGA/CPS/2015/006 – Preparation of functional inks for material inkjet printing and their applications in printed electronics and sensors – project investigator (head of the research team)

IGA/CPS/2016/007 – Preparation and characterization of functional polymer materials for thin films applicable in printed electronics and sensor technology – member of the research team

IGA/CPS/2017/008 – Preparation and characterization of nanocomposite thin films for polymer electronics – member of the research team

External funding

FR-TI3/424 Electroluminescent films for security interior lighting (2011-2014) – project researcher

NPU I LO1504 – Centre of Polymer Systems plus (2015-2020) – project researcher

CZ.01.1.02/0.0/0.0/15_019/0005090 – Stenopeic aperture for presbyopia correction (2016-2019) – project researcher

Jan Mašlík

**Preparation of Conductive and Semiconductive Patterns by
Digital Printing of Nanodispersions for Sensing Devices of
Organic Compound Vapours**

Příprava vodivých a polovodivých vzorů digitálním tiskem nanodisperzí pro
senzory par organických látek

Doctoral Thesis Summary

Published by: Tomas Bata University in Zlín,
nám. T. G. Masaryka 5555, 760 01 Zlín.

Edition: published electronically

Typesetting by: Jan Mašlík

This publication has not undergone any proofreading or editorial review.

Publication year: 2019

First Edition

ISBN 978-80-7454-849-9

